Four-probe charge transport measurements on individual vertically aligned carbon nanofibers

Lan Zhang,[a] Derek Austin,[b] Vladimir I. Merkulov, Anatoli V. Meleshko,[a] and Kate L. Klein[a]
Molecular-Scale Engineering and Nanoscale Technologies Research Group, Oak Ridge National Laboratory, P.O. Box 2008, MS 6006, Oak Ridge, Tennessee 37831

Michael A. Guillorn
Cornell Nanofabrication Facility, 250 Duffield Hall, Ithaca, New York 14853

Douglas H. Lowndes
Condensed Matter Sciences Division, Oak Ridge National Laboratory, Oak Ridge, Tennessee 37831

Michael L. Simpson[a),c)]
Molecular-Scale Engineering and Nanoscale Technologies Research Group, Oak Ridge National Laboratory, P.O. Box 2008, MS 6006, Oak Ridge, Tennessee 37831

(Received 11 December 2003; accepted 26 March 2004; published online 3 May 2004)

We report four-probe $I-V$ measurements on individual vertically aligned carbon nanofibers (VACNFs). These measurements were enabled by the fabrication of multiple Ti/Au ohmic contacts on individual fibers that exhibited resistance of only a few kilohms. These measurements demonstrate that VACNFs exhibit linear $I-V$ behavior at room temperature, with a resistivity of approximately 4.2×10^{-3} Ω cm. Our measurements are consistent with a dominant transport mechanism of electrons traveling through intergraphitic planes in the VACNFs. © *2004 American Institute of Physics.* [DOI: 10.1063/1.1748849]

Because of the ability of their controlled synthesis[1–5] and the ease of postgrowth processing,[6,7] vertically aligned carbon nanofibers (VACNFs) produced by plasma enhanced chemical vapor deposition (PECVD) are finding a variety of applications.[8–13] While many of these applications are concerned only with the structural or chemical properties of the VACNFs, detailed knowledge of nanofiber electrical properties is essential for many types of devices, including field emitters, electrochemical probes, and vertical electronic interconnects. Four-probe measurement of $I-V$ characteristics are essential for measuring inherent charge transport behavior, as the potentially large and nonlinear behavior of contact resistance limits the accuracy of two-probe measurements. Unfortunately, although two-probe measurements of VACNF charge transport have been published,[14–16] four-probe charge transport measurements for VACNFs have not yet been reported. In this letter, we report four-probe charge transport measurements made on individual VACNFs.

Forests of VACNFs were grown on silicon using dc PECVD as reported previously.[17] The height of VACNFs was 10 μm, and the diameter was approximately 150 nm. VACNFs were removed from the substrate by scratching with a needle and dropped onto a Si/SiO_2 chip on which alignment marks had been defined. The position of individual VACNFs was mapped relative to the alignment marks by scanning electron microscope (SEM) Hitachi 4700 observation. Poly(methylmethacrylate) (495 K, A8) was spun at 2300 rpm onto the substrate to achieve a thickness of 800 nm, and was then patterned by electron beam lithography and resist removal. After 12 s of reactive ion etch (RIE) (O_2 flow rate of 50 sccm, power 95 W), Ti (200 nm thick) and Au (200 nm thick) were deposited on the substrate, and lift-off was performed to leave patterned electrodes on the fibers. Usually five or more electrodes were patterned to assure successful four-probe measurements. Figure 1 shows a SEM image of a completed VACNF structure with five metal electrodes, the inset SEM image is the as-grown VACNF forest. Charge transport measurements were then performed using a precision semiconductor parameter analyzer (HP 4156A). All measurements were carried out in air at room temperature.

The sample preparation method described earlier allowed the measurement of inherent VACNF transport properties independent of junction effects between the substrate and VACNF.[13,14,16] However, this technique often leaves some resist residue at the VACNF sidewall surface, leading

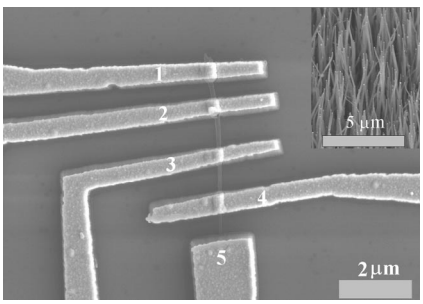

FIG. 1. A SEM image of a completed VACNF structure with five metal electrodes (200 nm each of Ti/Au) contacting the nanofiber. Inset is a SEM image of the as-grown VACNF forest.

[a)]Also at: Materials Science and Engineering Department, University of Tennessee, Knoxville, TN 37996.
[b)]Also at: Electrical and Computer Engineering Department, University of Tennessee, Knoxville, TN 37996.
[c)]Author to whom correspondence should be addressed; electronic mail: simpsonml1@ornl.gov

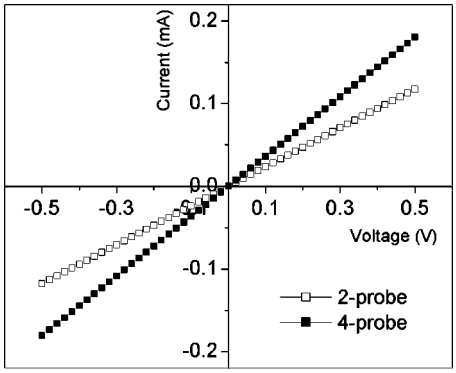

FIG. 2. $I-V$ curves for the four-probe (electrodes 1, 2, 3, and 4 of the device in Fig. 1) and two-probe (electrodes 2 and 3) measurements.

to errors in the subsequent electrical measurements. This problem may be exacerbated for PECVD grown VACNFs, whose structures are highly defective,[17] leading to high reactivity at the outer surfaces. The O_2 plasma RIE was used to remove this residue, allowing the formation of ohmic contacts with low contact resistance between the VACNF and metal electrodes. The etching time was optimized to avoid excessive O_2 plasma etching of the nanofibers. The effect of excessive O_2 plasma etching on the nanofiber structure will be addressed in a future publication. The typical resistance of contacts defined by this method was a few kilohms (kΩ). After successfully fabricating ohmic contacts with low contact resistance, four-probe charge transport measurements were carried out. The VACNFs exhibited linear $I-V$ behavior, as shown in Fig. 2. Two probe measurements on substrates without a nanofiber showed a leakage current in the picoampere range, and therefore had negligible effect on the transport measurements. The resistance of the segment of fiber between contacts 2 and 3 was 2.7 kΩ. The diameter and length of this fiber segment were approximately 135.5 nm and 0.880 μm, giving a fiber resistivity of 4.4×10^{-3} Ω cm ($\rho=R\times S/L$). A two-probe $I-V$ curve of this nanofiber segment is also included in this Fig. 2, from which the contact resistance of 1.3 kΩ was found. Measurements on 11 different fibers yielded similar results, with resistivity ranging from 3.2×10^{-3} Ω cm to 4.6×10^{-3} Ω cm (Fig. 3), and all

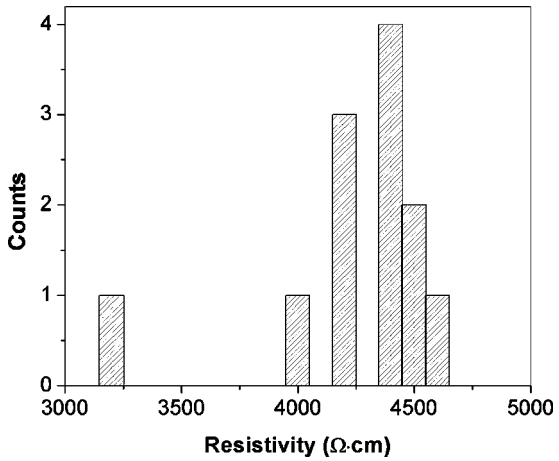

FIG. 3. Histogram of the four-probe measured resistivity of 12 VACNFs. The resistivity ranged from 3.2×10^{-3} Ω cm to 4.7×10^{-3} Ω cm. The average resistivity was 4.2×10^{-3} Ω cm.

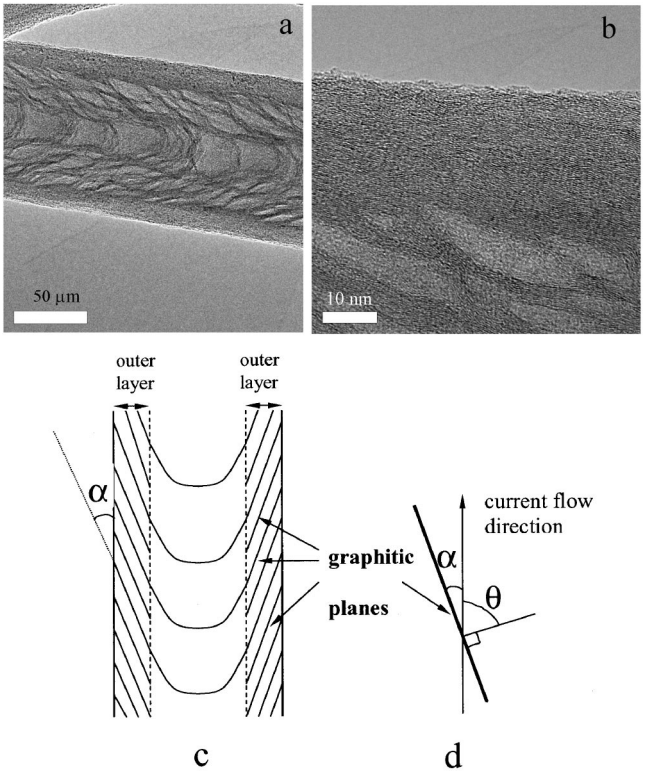

FIG. 4. (a) A transmission electron microscopy (TEM) image of a VACNF. VACNFs from the same forests in Fig. 1 were scratched by a needle and dropped onto a TEM grid. TEM (Hitachi, HF 2000) was used to determine the structure of individual VACNF. (b) A high-resolution TEM image of the outer layer of the VACNF in (a). The VACNFs possessed a ''herringbone'' and ''bamboo-like'' structure surrounded by a graphitic outer layer. The graphitic planes were not parallel to the fiber axis, but rather had an angle α to it. (c) A schematic representation of VACNF structure where α is the angle between the graphitic planes and the axis along fiber length. (d) The relationship between α and θ with $\theta=90°-\alpha$. The current flow is along the fiber length.

the $I-V$ curves (both two-probe and four-probe measured) were linear. The $I-V$ behaviors of the devices were carefully checked for gate effects using the heavily doped Si chip as a backgate. No effects were seen for gate voltages between -5 and 5 V, consistent with metallic VACNFs behavior.

The observation that the average VACNF resistivity (4.2×10^{-3} Ω cm) lies in between that of graphite parallel to the basal plane (4×10^{-5} Ω cm) and perpendicular to the basal plane (4×10^{-2} Ω cm) is consistent with a simple model of charge transport where electrons travel mainly from one graphitic plane to another along the length of the nanofiber. It is well known that VACNFs are composed of graphitic ''funnels'' and cones, in what is known as a ''herringbone'' and ''bamboo-like'' structure surrounded by an outer layer, as shown in Figs. 4(a) and 4(b). Figure 4(c) shows a schematic representation of such a structure. Applying a graphitic plane charge transport model to such a structure and taking the graphitic planes as the basal planes of graphite, resistivity is given by[17]

$$\rho(\theta)=\rho_a \sin^2\theta+\rho_c \cos^2\theta, \tag{1}$$

where θ is the angle of current flow to the axis perpendicular to the basal plane of graphite [Fig. 4(b)], ρ_a is the resistivity parallel to the basal plane, and ρ_c is the resistivity perpendicular to the basal plane. For our sample, θ was determined

to be 90°-α, where α is the angle between the graphitic planes and the fiber axis along the fiber length. α was shown in Figs. 4(a) and 4(b) to be about 20°, giving a θ of approximately 70°. For the values of ρ_a and ρ_c given earlier,[14] Eq. (1) yields $\rho = 4.7 \times 10^{-3}\ \Omega\,\mathrm{cm}$ for the nanofibers used here, in good agreement with our experimental measurements.

In conclusion, we successfully performed four-probe measurements on individual VACNFs by fabricating multiple ohmic contacts between VACNFs and Ti/Au electrodes, which had contact resistance of only a few kΩ. VACNFs exhibit linear $I-V$ behavior in air at room temperature with a resistivity of approximately $4.2 \times 10^{-3}\ \Omega\,\mathrm{cm}$. All our measurements are consistent with a model of transport within VACNFs dominated by travel between the graphitic planes along the length of the fiber.

The authors gratefully acknowledge funding support from the Material Sciences and Engineering Division Program of the DOE Office of Science, the DARPA Advanced Lithography Program under Contract No. 1868HH26X1 and the Laboratory Directed Research and Development Program of Oak Ridge National Laboratory. They are indebted to P. Fleming for assistance in electrode fabrication. This work was performed at the Oak Ridge National Laboratory, managed by UT-Battelle, LLC for the U.S. DOE under Contract No. DE-AC05-00OR22725.

[1] V. I. Merkulov, M. A. Guillorn, D. H. Lowndes, M. L. Simpson, and E. Voelkl, Appl. Phys. Lett. **79**, 1178 (2001).
[2] V. I. Merkulov, D. K. Hensley, A. V. Melechko, M. A. Guillorn, D. H. Lowndes, and M. L. Simpson, J. Phys. Chem. B **106**, 10570 (2002).
[3] V. I. Merkulov, A. V. Melechko, M. A. Guillorn, D. H. Lowndes, and M. L. Simpson, Appl. Phys. Lett. **80**, 476 (2002).
[4] V. I. Merkulov, A. V. Melechko, M. A. Guillorn, D. H. Lowndes, and M. L. Simpson, Chem. Phys. Lett. **350**, 381 (2001).
[5] Z. F. Ren, Z. P. Huang, J. W. Xu, J. H. Wang, P. Bush, M. P. Siegal, and P. N. Provencio, Science **282**, 1105 (1998).
[6] M. A. Guillorn, T. E. McKnight, A. Melechko, V. I. Merkulov, P. F. Britt, D. W. Austin, D. H. Lowndes, and M. L. Simpson, J. Appl. Phys. **91**, 3824 (2002).
[7] M. A. Guillorn, A. V. Melechko, V. I. Merkulov, E. D. Ellis, M. L. Simpson, L. R. Baylor, and G. J. Bordonaro, J. Vac. Sci. Technol. B **19**, 2598 (2001).
[8] L. R. Baylor, D. H. Lowndes, M. L. Simpson, C. E. Thomas, M. A. Guillorn, V. I. Merkulov, J. H. Whealton, E. D. Ellis, D. K. Hensley, and A. V. Melechko, J. Vac. Sci. Technol. B **20**, 2646 (2002).
[9] M. A. Guillorn, A. V. Melechko, V. I. Merkulov, E. D. Ellis, C. L. Britton, M. L. Simpson, D. H. Lowndes, and L. R. Baylor, Appl. Phys. Lett. **79**, 3506 (2001).
[10] T. E. McKnight, A. V. Melechko, G. D. Griffin, M. A. Guillorn, V. I. Merkulov, F. Serna, D. K. Hensley, M. J. Doktycz, D. H. Lowndes, and M. L. Simpson, Nanotechnology **14**, 551 (2003).
[11] A. V. Melechko, T. E. McKnight, M. A. Guillorn, D. W. Austin, B. Ilic, V. I. Merkulov, M. J. Doktycz, D. H. Lowndes, and M. L. Simpson, J. Vac. Sci. Technol. B **20**, 2730 (2002).
[12] L. Zhang, A. V. Melechko, V. I. Merkulov, M. A. Guillorn, M. L. Simpson, D. H. Lowndes, and M. J. Doktycz, Appl. Phys. Lett. **81**, 135 (2002).
[13] J. Li, Q. Ye, A. Cassell, H. T. Ng, R. Stevens, J. Han, and M. Meyyappan, Appl. Phys. Lett. **82**, 2491 (2003).
[14] J. Li, R. Stevens, L. Delzeit, H. T. Ng, A. Cassell, J. Han, and M. Meyyappan, Appl. Phys. Lett. **81**, 910 (2002).
[15] S.-B. Lee, K. B. K. Teo, M. Chhowalla, D. G. Hasko, G. A. J. Amaratunga, W. I. Milne, and H. Ahmed, Microelectron. Eng. **61–62**, 475 (2002).
[16] X. J. Yang, M. A. Guillorn, D. Austin, A. V. Melechko, H. Cui, H. M. Meyer III, V. I. Merkulov, J. B. O. Caughman, D. H. Lowndes, and M. L. Simpson, Nano Lett. **3**, 1751 (2003).
[17] B. T. Kelly, *Physics of Graphite* (Applied Science, 1981), p. 291.